Overview

Hydrogen related failure of steels – a new aspect

M. Nagumo

Recent studies of the characteristics and mechanism of hydrogen related failure in steels are overviewed. Based on an analysis of the states of hydrogen in steels, the role of hydrogen in reducing ductile crack growth resistance is attributed to the increased creation of vacancies on straining. Cases showing the involvement of strain induced vacancies in susceptibility to fracture are presented. The function of hydrogen is ascribed to an increase in the density of vacancies and their agglomeration, rather than hydrogen itself, through interactions between vacancies and hydrogen. The newly proposed mechanism of hydrogen related failure is supported by a recent finding of amorphisation associated with crack growth. **MST/6002**

Keywords: Steels, Hydrogen related failure, Physical modelling

Dr Nagumo (nagumo@waseda.jp) is Professor Emeritus, Department of Materials Science and Engineering, Waseda University, Tokyo, Japan. *Manuscript received 6 Octobert 2003; accepted 13 April 2004.*

Introduction

Premature failure or loss of ductility of steels caused by hydrogen has been the subject of many investigations for decades under terminologies such as hydrogen embrittlement, hydrogen induced or hydrogen assisted cracking and hydrogen related failure. The implications of these terminologies are somewhat different with respect to the nature of the phenomenon. Under high external hydrogen fugacity, the internal pressure of precipitated molecular hydrogen forms incipient cracks that trigger brittle fracture[1] or microvoids that link along shear bands.[2] On the other hand, under mild environments, the degradation is reversible by degassing without permanent defects remaining, thus suggesting that hydrogen intrinsically affects the lattice of materials.

The mysteries of hydrogen effects in steel that require causal explication include: a very small amount, less than one wt.ppm, of hydrogen induces failure; susceptibility to failure is highly sensitive to microstructures and compositions of steels even of the same strength level; unique fractographic features; and occasional time delays to fracture of days, months, and even years. In spite of extensive research studies documented in many review articles,[3–7] we have not yet obtained conclusive answers to these problems.

Difficulties in detecting hydrogen in connection with failure are due first to its presence in very small quantities, second to its low sensitivity to external excitations, and third to the high mobility of hydrogen atoms in steel. Recently, however, a substantial amount of work has been done in an effort to overcome these difficulties from new perspectives, particularly in recent projects conducted in Japan.[8,9] The present overview focuses on the function of hydrogen in the fracture process that is integral to the fundamental fracture modes.

States of hydrogen in steels and their detection

The solid solubility of hydrogen in the iron lattice follows Sievert's law and is endothermic in nature.[3] The equilibrium concentration of lattice hydrogen is as low as 2×10^{-8} in the atomic ratio at room temperature under one atmospheric pressure of hydrogen gas. Thus, most of the observed hydrogen is in trapped states at various lattice defects, the binding energies of which with hydrogen are given in the literature.[3,10,11] Hydrogen absorption becomes exothermic in deformed iron.[12] Differences in hydrogen absorption among steels under the same hydrogen charging condition originate in differences of the trapping sites. However, the assignment of trapping sites is not always straightforward, particularly in steel, because of complicated microstructures.

Visualisation of hydrogen is useful for revealing its local distribution, and several techniques have been developed for this purpose. Tritium autoradiography, which utilises the decomposition of silver halides by β-rays, successfully revealed the accumulation of tritium along slip bands as well as along grain boundaries and second phase particles.[13–16] However, the detected tritium is in most cases strongly trapped, since mobile tritium is degassed for safety prior to emulsion coating. Another method is the hydrogen microprint technique (HMT), which utilises the reduction of silver ions by hydrogen to metallic silver.[17] It is useful for detecting mobile hydrogen in addition to being convenient to use under ambient atmosphere. Recent improvements in spatial resolution and detection efficiency have revealed enhanced hydrogen diffusion under a stress gradient and accumulation at stress concentrated areas.[18,19]

While visualisation gives intuitive views regarding the trapped states of hydrogen, it generally lacks quantitative or atomic scale information. For that reason, hydrogen thermal desorption analysis (TDA) has been employed to investigate the trapped states.[20,21] Upon heating, hydrogen contained in a sample is thermally desorbed, and from the associated desorption rate peak(s) the tapped states can be analysed.

Two types of rate determining step for the evolution of a TDA peak exist depending on the type of trapping involved. In the case of strongly trapped hydrogen,[20] a desorption peak on heating appears as the result of an increase in thermal dissociation and a decrease in the amount of trapped hydrogen. In general, multiple desorption peaks appear corresponding to the respective trapped states. In TDA of hydrogen charged to a cold drawn pure iron, a single peak appeared as shown in Fig. 1*a*,[22] which subsequently disappeared after keeping the specimen at room temperature for 48 h, implying the weakly trapped nature of hydrogen. On the other hand, two desorption peaks appeared in a eutectoid steel given the same amount of cold drawing, as shown in Fig. 1*b*.[22] The higher temperature peak in Fig. 1*b* remained after the hydrogen charged specimen was kept for over 24 h at room

 DOI 10.1179/026708304225019687

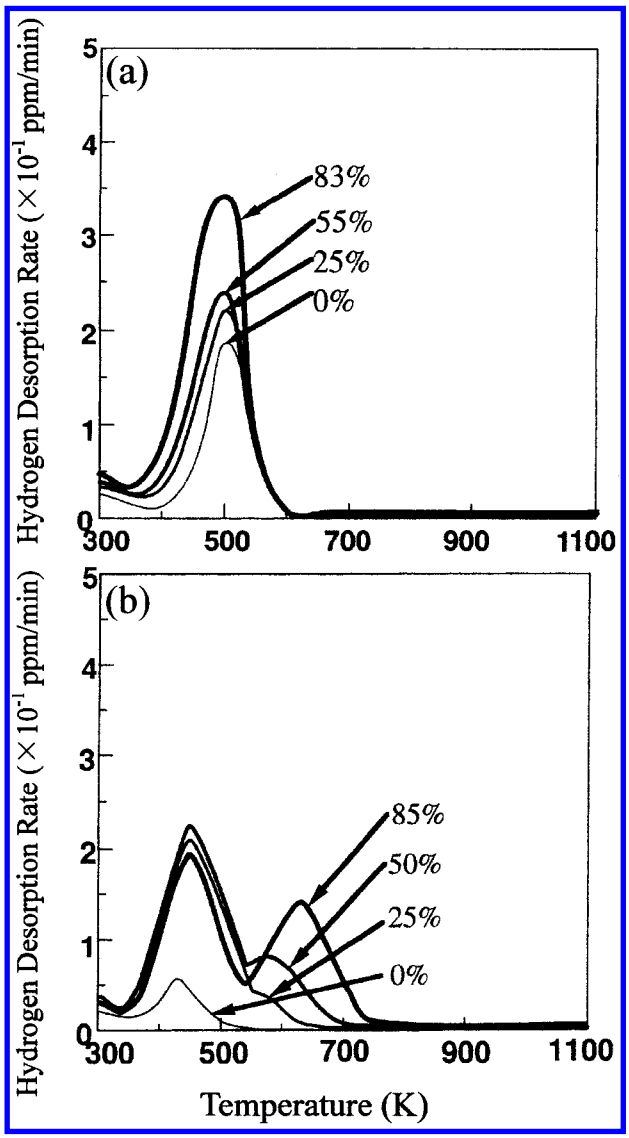

a pure iron; *b* eutectoid steel subjected to increased reduction by cold drawing

1 TDA curves of hydrogen introduced to two different metals The % values denote the reduction in cross sectional area

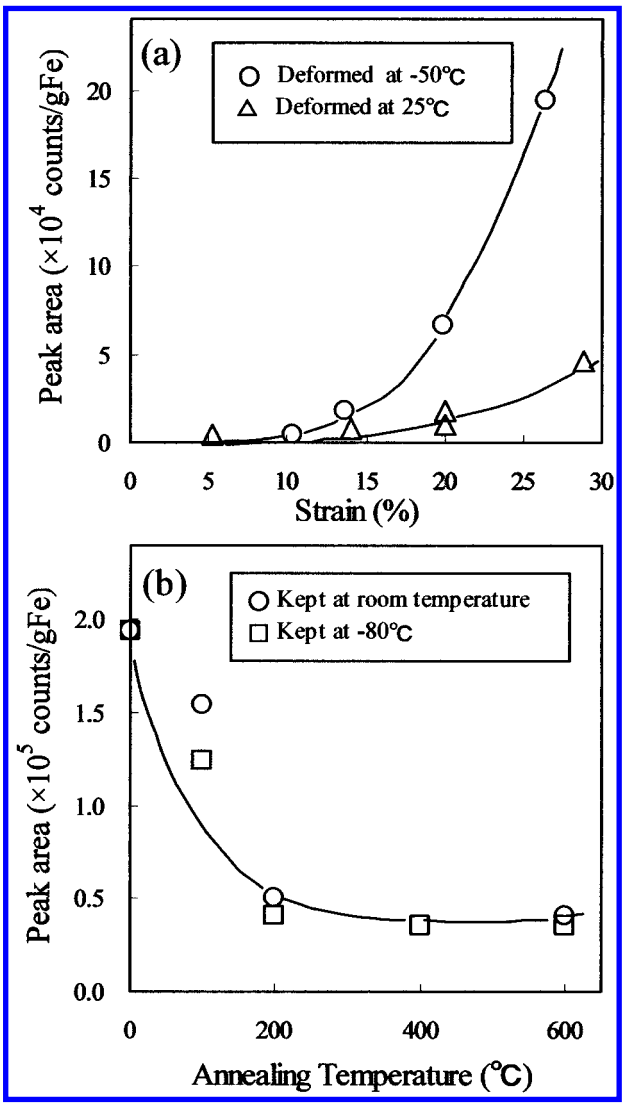

2 *a* hydrogen absorption capacity in a ferritic steel subjected to tensile straining at different temperatures; *b* reduction in hydrogen absorption capacity shown in *a* by annealing after straining

temperature, suggesting a strongly trapped hydrogen state. The two types of hydrogen are fairly well separated experimentally by keeping hydrogen charged specimen at room temperature for a substantial period.

For weakly trapped hydrogen, reversible to lattice hydrogen under a local equilibrium, the evolution of a desorption peak is the result of the enhanced diffusion rate of hydrogen and a decrease in the total amount of hydrogen in the specimen. Using the formula of the hydrogen diffusion constant given by Oriani,[23] the observed desorption peak profiles were successfully simulated by a proper choice of the trap density and binding energy.[24] With increasing trap density and binding energy, the peak temperature shifts to a higher level, the latter being more effective for the shift. Experimentally, the peak temperature is often observed to vary with specimen size, which is the case of weakly trapped hydrogen. The disappearance of the peak in Fig. 1*a* and the lower temperature peak in Fig. 1*b* as a result of keeping the specimens at room temperature indicate that hydrogen constituting the peaks is weakly trapped. It is to be noted that Oriani's formula presumes the hydrogen occupancy of defects is much less than unity. The agreement of the observed desorption curves with calculated ones implies that the actual defect density can be substantially higher than that estimated from the hydrogen concentration assuming equiatomic correspondence.[24]

A useful application of TDA is to use hydrogen to probe defects in materials. By introducing hydrogen into materials and observing its desorption behaviour, we can detect atomic scale defects. Figure 2*a*[25] indicates the amount of tritium absorbed in plastically deformed ferritic iron as a function of the amount of strain. The amount of absorbed tritium increased with strain, implying the formation of trapping defects by straining. A noteworthy finding was the increase in absorption when the material was deformed at a lower temperature even to the same amount of strain and its concave dependence on strain. Further, when the deformed specimens were subjected to annealing, as shown in Fig. 2*b*,[25] the increase in tritium absorption was reduced by annealing at temperatures as low as 200°C where the decrease in dislocation density was not expected, indicating the pointlike nature of the defects, presumably vacancies. Similar behaviour has also been reported in martensitic steels.[26] An important finding with regard to the effect of hydrogen was that the increase in hydrogen absorption capacity by plastic straining was enhanced when the material was deformed in the presence of hydrogen.[27]

The assignment of strain induced defects to vacancies by means of hydrogen TDA, however, is indirect. Recently, positron lifetime spectroscopy has been applied for identifying strain induced defects and the function of hydrogen.[28] The mean positron lifetime τ_m in a pure iron increased from about 100 ps in an annealed specimen, the lifetime in the iron lattice, to about 120 ps and 130 ps when tensile strained to 10 and 20%, respectively, due to the formation of lattice defects, dislocations together with vacancies. When hydrogen was precharged, τ_m was not affected in the non-deformed specimen, but τ_m for the respective amount of strain further increased to 128 ps and 145 ps, indicating enhanced creation of defects. A multicomponent analysis of positron lifetime spectrum showed the existence of vacancy clusters that may correspond to a decrease in τ_m at around 100°C on isochronal annealing experiment. The results are consistent with those of TDA that inferred the creation of vacancies and their clusters during plastic straining, enhanced by the presence of hydrogen. While positron lifetime measurement detected the increase in dislocation density, TDA was rather immune to dislocations. The reason is for further studies.

Characterisation of fracture process

The function of hydrogen in the fracture process is to favour either the tensile separation of atomic bonds or the shear off of ligaments. The former is the case of brittle fracture. Griffith's condition is the criterion for the onset of unstable fracture, and hydrogen effects appear either as the formation of an incipient crack or as a reduction of the effective surface energy. Shear off is an example of ductile fracture that proceeds with the formation of microvoids followed by their growth and linking, where hydrogen affects void initiation and/or linking processes.

FRACTOGRAPHIC FEATURES

Toughness and tensile properties are the results of various steps leading to fracture, which appear in fractographic features. While cleavage fracture induced by a high internal hydrogen pressure has occasionally been observed, characteristic fractographic features of hydrogen related failure are striations and quasicleavage patterns. Figure 3 shows micrographs of the tensile fractured surface of a polycrystalline hydrogen charged iron.[29] The striations in Fig. 3*a* are along the traces of {110} or {112} slip planes, occasionally associated with void formation. In a grain with a different orientation to the tensile axis, the pattern shown in Fig. 3*b* is a so called quasicleavage that is also often observed in hydrogen charged martensitic steels. Terasaki *et al.* examined the fracture surface of a hydrogen charged Fe–3 wt-%Si steel single crystal specimen oriented [001] parallel to the tensile axis.[30] The fracture was apparently along the (100) plane, but fine striations along {112} were also revealed. While the main crack propagation was to [010], an AFM observation revealed microvoid arrays at intersections of the $(\bar{1}12)$ and (112) striations. Their conclusion was that the void initiation due to hydrogen takes place at slip bands or cell walls and that the linking of voids leads to crack growth even though the macroscopic fracture plane is (001). Marrow *et al.* also observed a similar fine striation pattern,[31] but it was attributed to dislocation trails formed by dislocation loops nucleated ahead of a propagating cleavage crack.

DUCTILE CRACK GROWTH RESISTANCE

While fractography provides useful information about the crack path, the crack growth resistance that is directly related to tensile properties must be examined. In the ductile–brittle fracture transition temperature region, ductile crack growth precedes the initiation of unstable brittle fracture. The resistance curve (R-curve) that denotes the J-integral versus advanced crack length is a useful tool for analysing the effect of microstructures and also that of hydrogen in the fracture process. Void initiation in ductile fracture has been thought to occur primarily at second phase particles. However, some observations have revealed a dimple pattern without second phase particles and symptoms of vacancy agglomerations.[32–35]

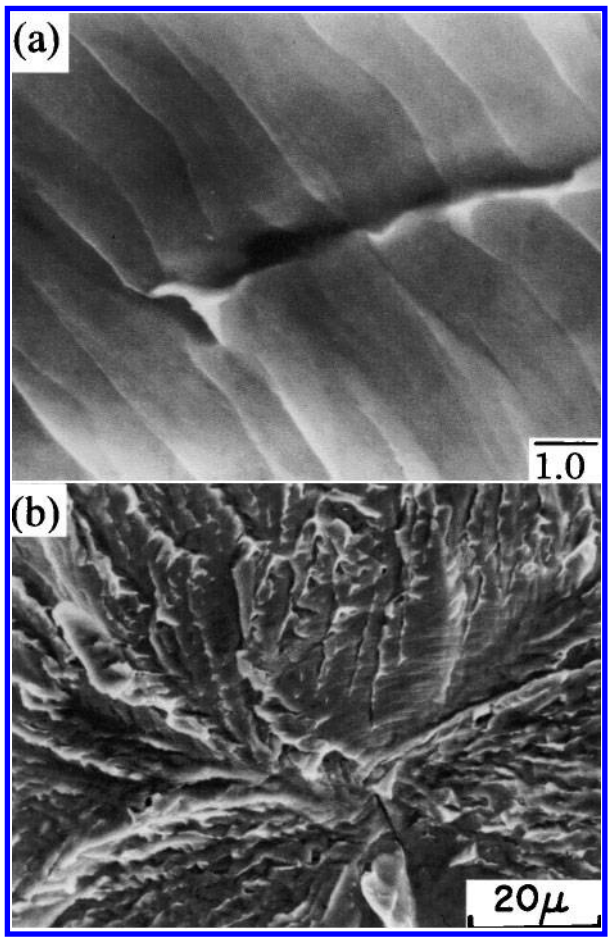

a striated; *b* quasicleavage

3 Features of tensile fractured hydrogen charged polycrystalline iron

Figure 4 shows the R-curves obtained by means of a three point bending test using fatigue notched specimens of three low carbon ferritic steels.[36,37] The steels are of similar strength and microstructures with their only difference being in the fraction of cementite or pearlite along ferrite grain boundaries that act as constraint phases against slip extension. The resistance against ductile crack growth, denoted as the slope of the R-curve, is plotted in Fig. 5 as a function of the constraint factor defined as the ratio of the grain boundary length with constraint phases to the total boundary length.[37] It is evident that the increased fraction of the constraint phases reduces crack growth resistance. The use of hydrogen as a probe for defects was then applied to investigate the origin of the reduction. Figure 6 shows in the ordinate the amount of tritium absorbed in specimens given 20% plastic strain at different temperatures.[36] The increase in the hydrogen absorption capacity with the constraint factor and its dependence on deformation temperature imply that the increase in the constraint factor creates a higher density of defects, presumably vacancies. The effect of the constraint factor on defect

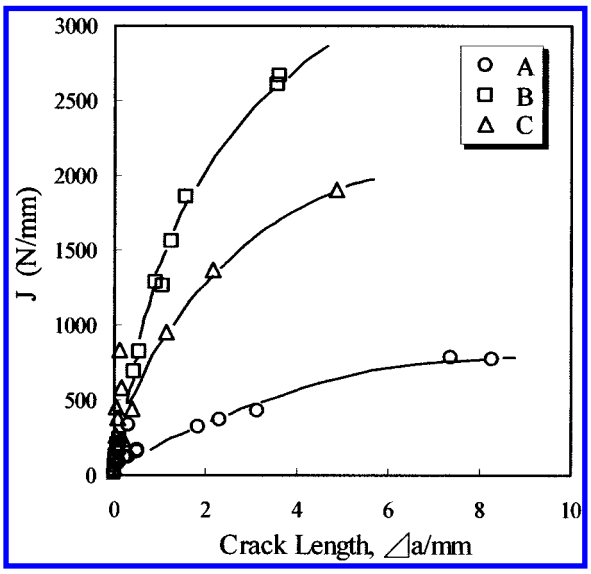

4 Ductile crack growth resistance curves (R-curves) of three experimental steels. Δa is the crack length measured from the original precrack front: R-curves obtained in three point bending test using fatigue notched specimen

formation is shown in Fig. 7, which shows the time decay of absorbed tritium.[36] When the specimens were in the undeformed state, the difference among the three steels was negligible, but the diffusion of tritium was more retarded in the steels with higher constraint factors when plastic straining of 20% was applied. Figure 7 also indicates the formation of a higher density of defects that stably trap hydrogen in the steels with higher constraint factors. Figures 5 and 6 present the first finding that showed a decrease in crack growth resistance due to the enhanced formation of defects on straining.

EFFECT OF HYDROGEN

The technique of R-curve analysis has been used to reveal hydrogen effects on the fracture process. The same steels as those used in Figs. 4–7 were hydrogen charged and subjected to testing. Hydrogen was precharged by means of cathodic electrolysis under a rather mild condition so as

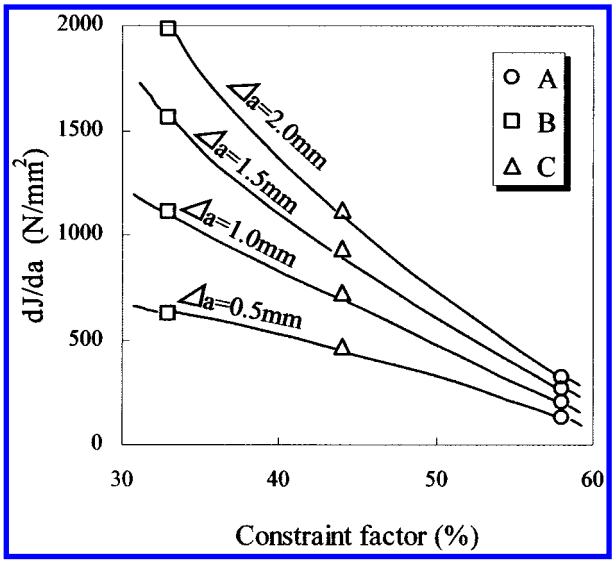

5 Decrease in crack growth resistance d*J*/d*a* at different crack lengths associated with increasing constraint factor of steels shown in Fig. 4

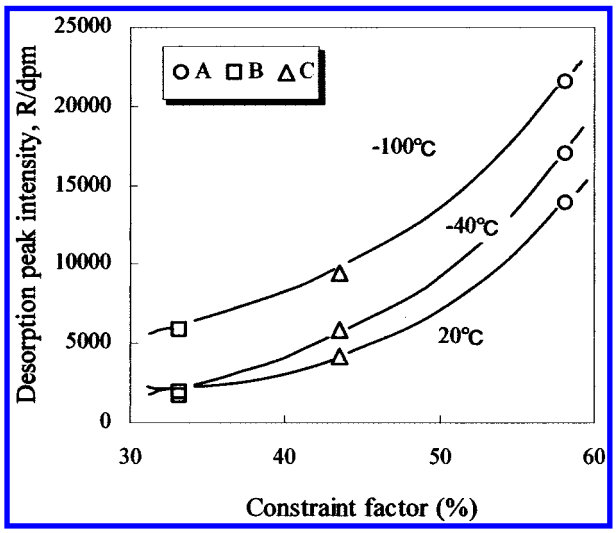

6 Increase in tritium absorption capacity associated with increasing constraint factor of steels in Fig. 4, strained to 20% at different temperatures

not to cause damage on charging, i.e. using 3%NaCl aqueous solution added 3 g L^{-1} NH_4SCN under a current density of 5 A m^{-2} for 24 h. Figure 8 compares the R-curves of a steel with and without hydrogen charging, showing a decrease in ductile crack growth resistance attributable to hydrogen.[38] The circles and triangles are the experimental and calculated J-integral values, respectively. The calculations were performed by means of a finite element method (FEM) using Gurson's model, which comprises the void volume fraction in the constitution equation of the elements.[39] For the hydrogen free specimen, good agreement between the calculated and observed R-curves was obtained by using the experimentally observed flow stress and void volume fraction as parameters for the calculation. For the hydrogen charged specimen, the observed R-curve was reproduced by increasing the initial void volume fraction from 2 to 3·5%. The FEM calculations also showed a more prominent localisation of both the nucleation and total voids at the crack tip for a higher initial void volume fraction.[38]

The localisation of voids at the crack front was consistent with fractographic features in terms of a histogram of the aspect ratio of dimples, i.e. the depth to width ratio in specimens with/without hydrogen charging, as shown in

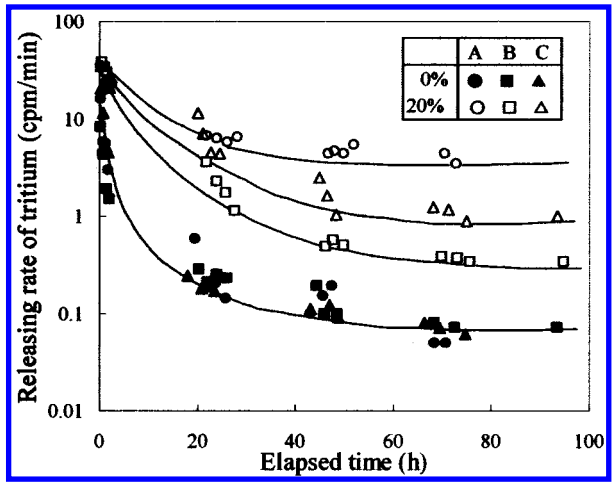

7 Tritium desorption at room temperature from steels in Fig. 4, either non-deformed or strained to 20% at room temperature

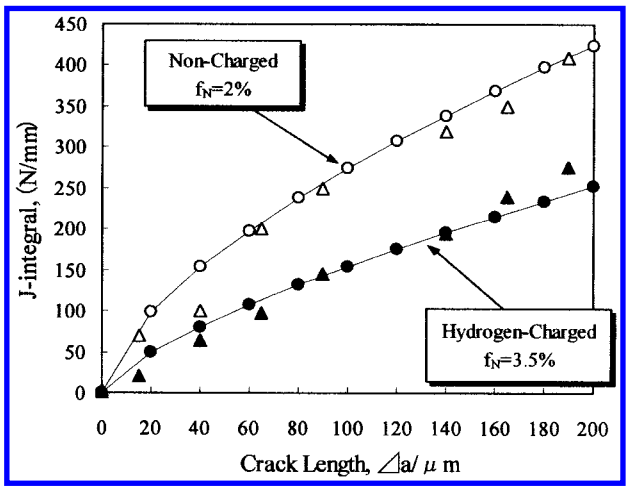

8 Ductile crack growth resistance curves (R-curves) of steel B of Fig. 4 with/without hydrogen charging: ○, ● experimental data; □, ▲ FEM calculations; hydrogen was precharged by means of cathodic electrolysis under mild conditions so as not to cause damage on charging, i.e. using 3%NaCl aqueous solution added to 3 g L^{-1} NH_4SCN under a current density of 5 A m^{-2} for 24 h

Fig. 9.[38] In the hydrogen charged specimen, dimples tended to be shallow, implying less energy dissipation per unit distance of crack advance. Quasicleavage like patterns were observed at the bottom of dimples. Using the same steel as that used in Fig. 4, HMT and tritium autography were successfully applied to reveal the strain induced formation and agglomeration of vacancies and their localisation in strain concentrated areas as well as along grain boundaries that act as constraints against slip extension.[40]

If one of the controlling factors of ductile crack growth resistance is the formation of defects during plastic deformation as seen in Figs. 5–7, the implication of Fig. 8 is that the effect of hydrogen in the fracture process is to enhance the formation of voids that provide an easy path for crack growth. This concept is in accord with the increase in hydrogen trapping defects when deformation takes place in the presence of hydrogen.[27] Creation of a high density of vacancies far exceeding the thermal equilibrium values has been shown experimentally and theoretically as a consequence of reduced formation energy of vacancies by combining with hydrogen.[41–44]

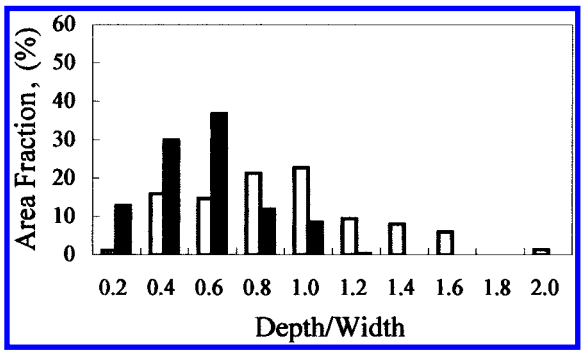

9 Area fractions of dimples with different depth/width ratio in steel B of Figs. 4–7 tested with/without hydrogen precharging: open and solid symbols indicate non-charged and hydrogen charged samples, respectively

Mechanism of hydrogen related failure

The mechanism of hydrogen related failure has been an issue of extensive research for decades. Figure 10 positions major current theories according to the hydrogen states they presume. As described previously, the precipitation of molecular hydrogen at second phase particles eventually forms microcracks under high fugacity of external hydrogen and explains crack propagation in a brittle manner. One feature of hydrogen related failure is the promoted plastic instability in the form of shear localisation. The hydrogen enhanced autocatalytic process, voids promoting shear localisation and following shear localisation promoting void formation, has been proposed by Hirth.[45] The role of hydrogen was assumed to enhance particle decohesion or cracking at second phase particles, while hydrogen may contribute to localised deformation in the near crack tip plastic zone.

Against the predominance of strongly trapped hydrogen in failure, an important finding was that a hydrogen charged cold drawn eutectoid steel was immune to a sustained loading delayed fracture test after degassing easily diffusive hydrogen by keeping the specimen at room temperature, where strongly trapped hydrogen, i.e. the higher temperature TDA peak in Fig. 1*b*, still remained.[46] Other studies also suggested that easily diffusive hydrogen is essential for the occurrence of failure at least under mild environments.[46–48] Easily diffusive hydrogen consists of lattice hydrogen and weakly trapped hydrogen. The lattice

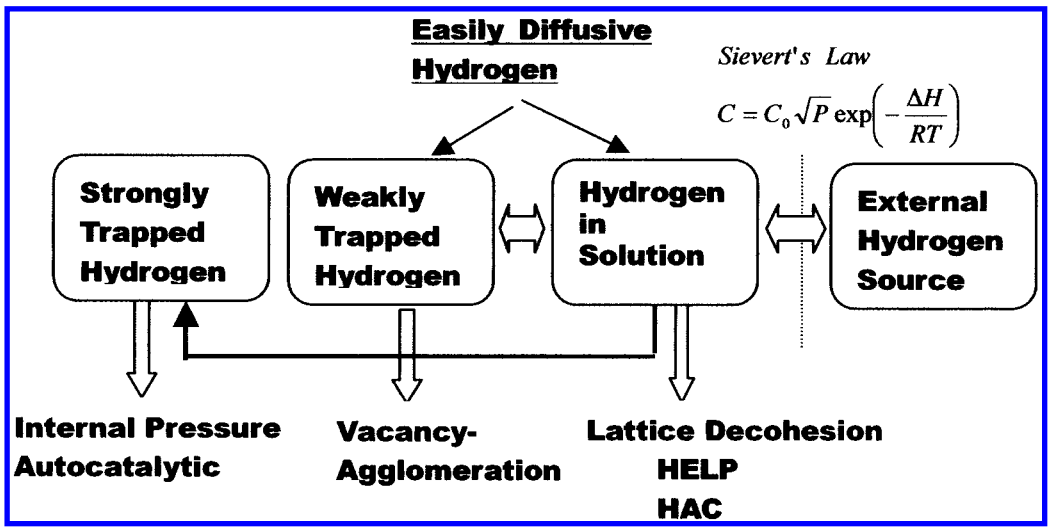

10 Outline of proposed mechanisms of hydrogen related failure with respect to hydrogen states in steel

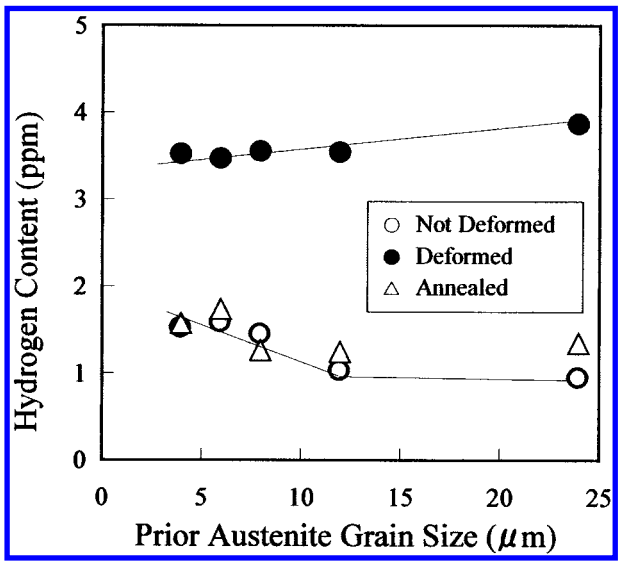

11 Hydrogen absorption capacity of martensitic steel with different prior austenite grain sizes; non-deformed, deformed to 5% and annealed at 250°C for 1 h after straining

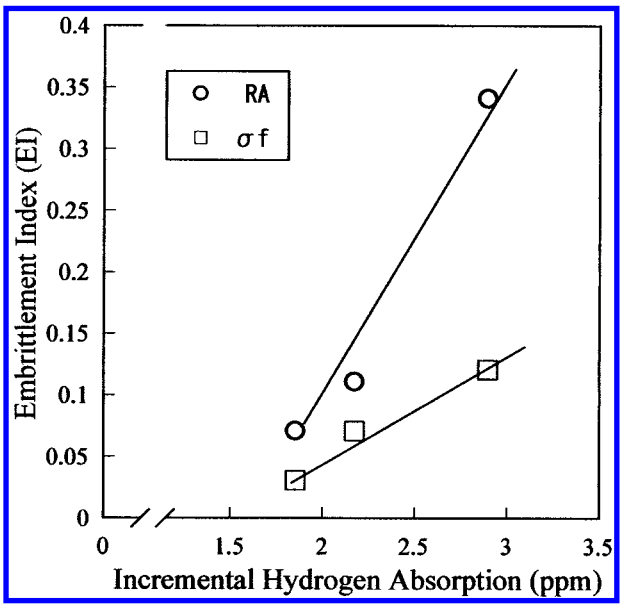

12 Relationship between embrittlement index *EI*, defined as the fraction of the decrease in reduction in area *RA* or fracture stress σ_f, and amount of strain induced increase in hydrogen absorption of steel in Fig. 11: slow strain rate tensile test conducted using flat specimens 2 mm thick, 10 mm wide at strain rate 3×10^{-5} s^{-1}; hydrogen precharging was by means of cathodic electrolysis using a 3%NaCl aqueous solution added to 3 g L^{-1} NH_4SCN under a current density of 10 A m^{-2} for 21 h

decohesion theory presumes the function of lattice hydrogen in reducing atomic bond strength.[49–51] While a decrease in Fe–Fe bond strength is plausible by charge transfer from Fe atoms to surrounding H atoms,[52] experimental evidence supporting lattice decohesion by hydrogen has never been reported. The hydrogen enhanced localised plasticity (HELP) theory is based on a series of observations for various metals and alloys by means of *in situ* transmission electron microscopy that revealed accelerated mobility of dislocations under a hydrogen atmosphere.[6,53] Theoretically, a hydrogen atmosphere formed at dislocations reduces the interaction energy between the dislocation–hydrogen complex and other elastic centres, resulting in increased dislocation mobility and shear localisation at regions of high hydrogen concentration.[53,54] One problem might be that a substantial density of lattice hydrogen, around 10^{-3} in atomic ratio, is needed in order to markedly reduce the elastic energy of dislocations.[55] Lynch has suggested another mechanism for HELP from a viewpoint based on surface effects on dislocation dynamics.[4]

Both the lattice decohesion and HELP theories presume the function of lattice hydrogen. Since the solid solubility of hydrogen in iron, given by Sievert's law, is extremely low,[3] a substantial accumulation of hydrogen must be assumed. Stress fields at the crack tip and other elastic singularities are possible sites,[56–58] but a high concentration exceeding the average concentration by more than one order of magnitude has never been observed.

A viewpoint so far disregarded is the function of weakly trapped hydrogen in Fig. 10. The findings shown in Fig. 2 and the recent positron lifetime measurement[28] indicate the formation of a substantial density of vacancies on plastic deformation, and Figs. 5 and 6 show their connection with crack growth resistance.

A series of experiments conducted recently have changed the viewpoint on hydrogen related failure from some intrinsic effect of hydrogen itself to vacancies the creation of which hydrogen is involved in.

Relation of strain induced vacancies to susceptibility to hydrogen related failure

A subject we have to elucidate is the function of the microstructures and compositions of steels on susceptibility to hydrogen related failure. Grain refinement is a major current in modern steel technology, and its effect on hydrogen related failure has been examined with a martensitic steel.[59] A 0·36 wt-%C steel was subjected to repeated induction heating and quenching to promote austenite grain refinement, followed by tempering at 550°C to the tensile strength of 1360 MPa. Figure 11 shows the hydrogen absorption of specimens with different grain sizes, as heat treated, strained to 5%, and annealed after straining at 250°C for 1 h. The hydrogen absorption capacity increased by refining the grain size to less than 10 μm due to the increase in the grain boundary area. In accord with previous results,[27] plastic straining substantially increased the hydrogen absorption capacity, but the total amount, on the contrary, showed a decrease with grain refinement. Subsequent annealing after straining totally reduced the increase, showing the point defect like nature of the resultant defects that act as increased trap sites of hydrogen. Susceptibility to hydrogen related failure by means of a slow strain rate tensile test was evaluated in terms of the embrittlement index *EI*, defined as the fraction of the decrease in reduction in area *RA* or fracture stress σ_f. The suffix H or A denotes a specimen tested with/without hydrogen precharging, respectively.

$$EI_{RA}=\frac{RA_A-RA_H}{RA_A},\qquad EI_{\sigma_f}=\frac{\sigma_{fA}-\sigma_{fH}}{\sigma_{fA}}$$

The slow strain rate tensile test was conducted using flat specimens 2 mm thick and 10 mm wide at a strain rate of 3×10^{-5} s^{-1}. Hydrogen precharging was by means of cathodic electrolysis using a 3%NaCl aqueous solution containing 3 g L^{-1} NH_4SCN under a current density of 10 A m^{-2} for 21 h. Figure 12 shows the dependence of EI on the increment of hydrogen absorption, i.e. the amount of strain induced defects. Together with the annealing effect shown in Fig. 11, Fig. 12 implies that susceptibility is closely related to the density of strain induced defects, presumably vacancies.

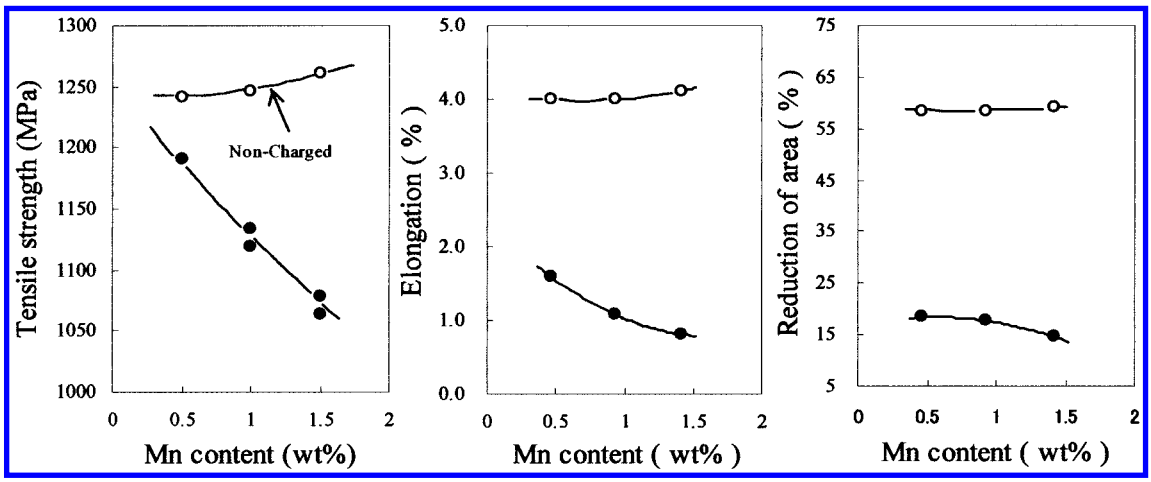

13 Tensile test results for steels with different manganese content under concurrent hydrogen charging: ○ without hydrogen charging, ● with hydrogen charging; slow strain rate tensile test was at $5{\cdot}6\times10^{-6}$ $s^{-1}$and hydrogen charging was by means of cathodic electrolysis using a 3%NaCl aqueous solution added 0·5 g L^{-1} NH_4SCN under a current density of 5 A m^{-2}

A similar correlation between susceptibility to failure and the amount of strain induced defects was observed in martensitic steels that showed intergranular mode fracture.[60] Steels of 0·30 wt-%C and varied amounts of manganese were subjected to a slow strain rate test under concurrent hydrogen charging. The strain rate was $5{\cdot}6\times10^{-6}$ s^{-1} and hydrogen charging was by means of cathodic electrolysis using a 3%NaCl aqueous solution containing 0·5 g L^{-1} NH_4SCN under a current density of 5 A m^{-2}. As shown in Fig. 13,[60] a pronounced degradation of tensile properties appeared under hydrogen charging with increasing manganese content. Hydrogen absorption capacity of deformed samples is shown in Fig. 14, hydrogen being used as a probe for defects.[25,60] While hydrogen absorption capacity was unrelated to manganese content in the undeformed state, it increased associated with the application of plastic straining more noticeably in steels with a higher manganese content. The increase in hydrogen absorption capacity due to straining was ascribed to the density of point defects, since it recovered when annealed at 250°C. Figure 15 shows the hydrogen TDA curves of the 1·5 wt-%Mn steel specimens subjected to straining to 2% and annealed after straining.

The fracture mode was intergranular with tear traces along martensite lath boundaries, as shown in Fig. 16,[60] but the tear traces and the average surface roughness decreased with increasing manganese content. The results are consistent with previous findings that revealed the role of slip constraints in crack growth resistance. The role of manganese is not definite, but a higher content of manganese may enhance the constraints through the precipitation of carbides and/or segregation of manganese along grain boundaries.

Besides the correlation between susceptibility to failure and the amount of strain induced hydrogen absorption, the effect of the microstructure appeared in the thermal desorption curve profile. The susceptibility of a 0·33 wt-%C martensitic steel to a sustained loading delayed fracture under a corrosive environment, immersed in an aqueous solution of 20 wt-%NH_4SCN kept at 50°C, was reduced when tempered at higher temperature, as shown in Fig. 17.[27] The increase in hydrogen absorption appeared again when the specimens were preloaded, but it was more conspicuous under concurrent loading/hydrogen charging. This finding implies that hydrogen enhances the formation

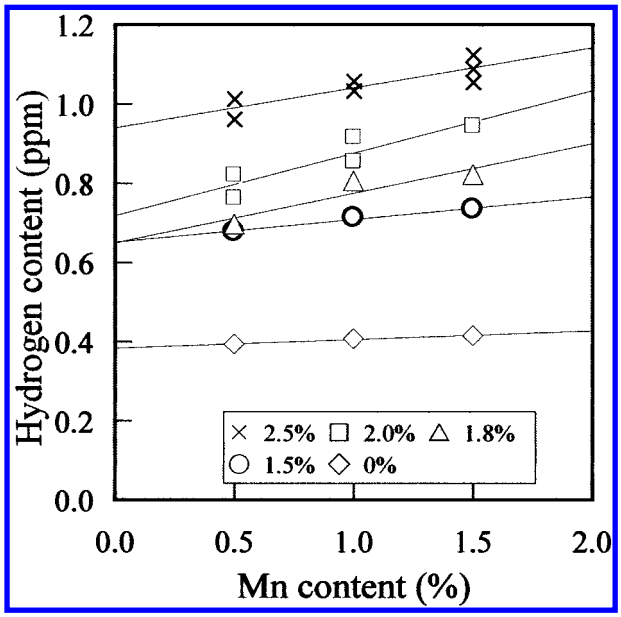

14 Increase in hydrogen absorption capacity with manganese content. Various amounts of prestrain applied prior to hydrogen charging

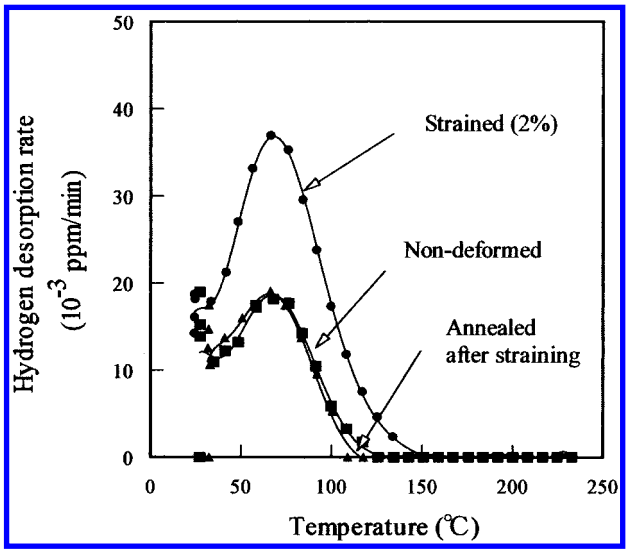

15 Hydrogen TDA curves of 1·5 wt-%Mn steel specimens; non-deformed, prestrained to 2%, and annealed at 250°C for 1 h after straining

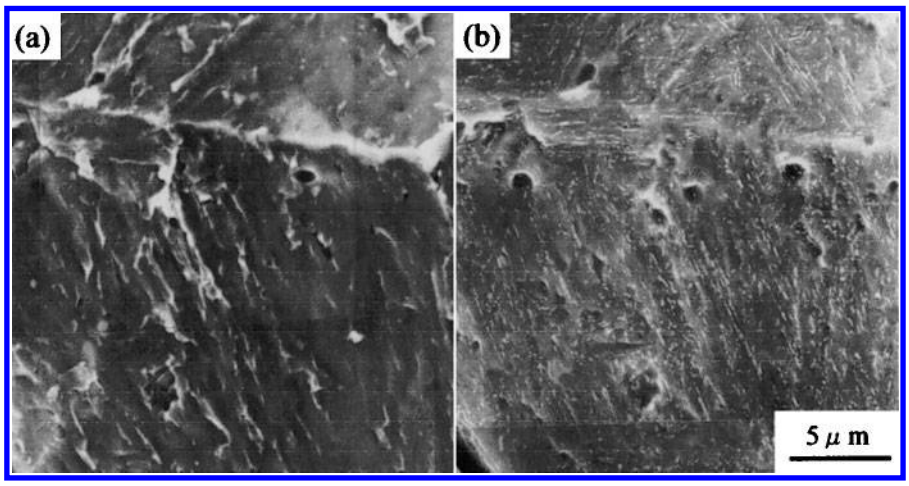

a before chemical etching; *b* after chemical etching

16 Intergranular fracture surface of 0·5%Mn steel showing correspondence of tear patterns with martensite lath structures

of defects during loading. As hydrogen entry proceeded, as shown in Fig. 18,[27] the increment, which appeared initially in the low temperature region of the original TDA peak, was reduced and appeared in the higher temperature region. The alteration occurred earlier in steels tempered at lower temperatures with a higher susceptibility, as shown in Fig. 19.[27] The shift of the desorption peak to higher temperatures implies the evolution of trap sites with a higher binding energy with hydrogen. Vacancy agglomeration was assumed as a probable reason. According to the rate theory, a higher production rate of aggregates owing to a higher density of monovacancies was considered, being consistent with the case of the correlation between the amount of strain induced defects and susceptibility shown in Figs. 12 and 14.

The alteration of the TDA peak profile associated with susceptibility to failure was also observed in a martensitic steel subjected to a delayed fracture test for which the hydrogen charging current density was cyclically alternated.[61] The time to fracture was reduced by increasing the frequency of the current alternation as shown in Fig. 20.[61] In that experiment, cyclic variation of the current density was a rectangular form in which the maximum current density was constant in order to eliminate the effect of excess current density on the failure. The amount of

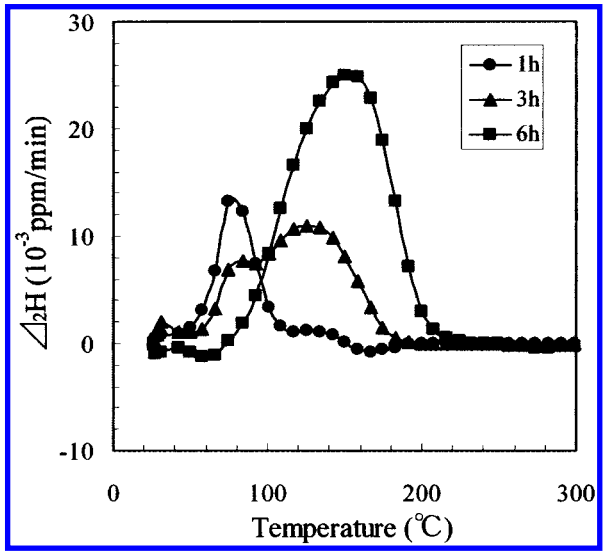

18 Dependence of incremental hydrogen desorption due to concurrent charging/loading on immersion time: specimens tempered at 250°C

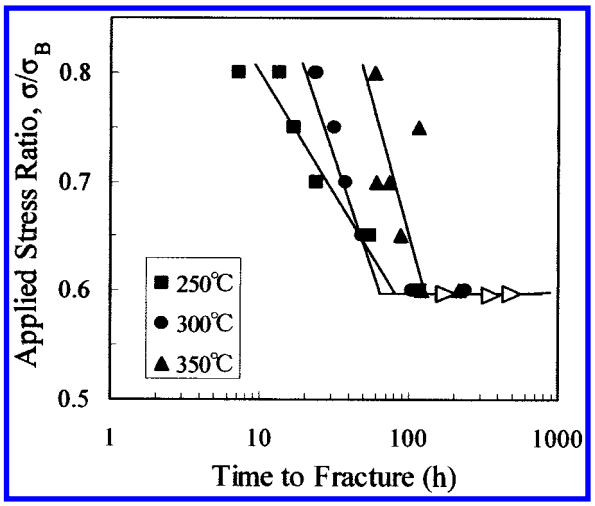

17 Delayed fracture diagram of martensitic steels tempered at different temperatures: test in an aqueous solution of 20 wt-%NH_4SCN at 50°C; arrows denote non-failed samples

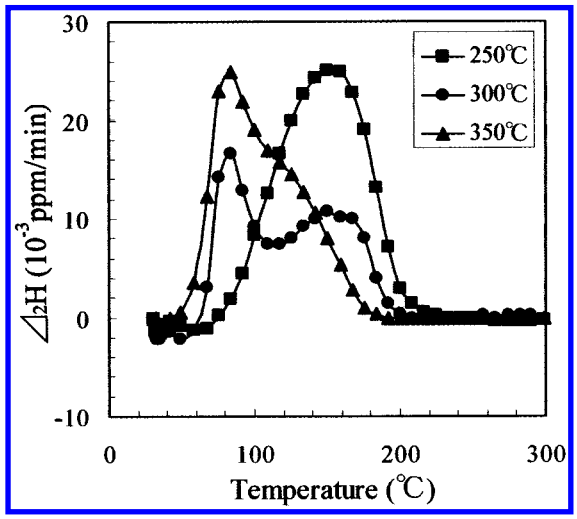

19 Comparison of incremental hydrogen desorption of specimens tempered at different temperatures subjected to concurrent charging/loading at an immersion time of 6 h

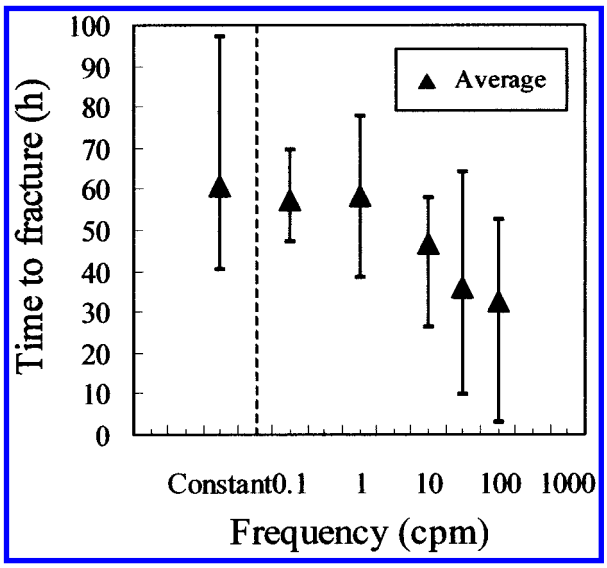

20 Time to fracture in a sustained loading delayed fracture test as function of frequency of supplied cyclic current

absorbed hydrogen was uniquely determined by the supplied electric charge. Then, the earlier fracture under cyclic current took place with less hydrogen content than that under the constant current condition. In this case, desorption on the lower temperature side and also the following increase in the higher temperature side of the TDA peak were prominent in the alternate charging condition. The function of cyclic alternation of the charging current was tentatively assumed to increase the frequency of combination/dissociation of hydrogen/defect complexes through the change in the solid solubility of hydrogen, thus increasing the chance of forming new couples that grow to stable agglomerates.

An important implication of the last case is that hydrogen content is not always the decisive quantity that determines the failure of a specific steel, but the tendency to create vacancies on straining is essential for such susceptibility. In this respect, the stability of dislocation configurations, an expected result of tempering martensitic steels, has been considered as an essential factor, and stress relaxation was employed as a measure of the stability with a Mo–V martensitic steel.[62] Susceptibility to a delayed fracture was reduced when tempered at 650°C, where precipitation of fine carbides took place, compared with tempering at 550°C, while hydrogen absorption capacity increased associated with carbide precipitation. The stress relaxation of the specimen tempered at 650°C was smaller than that tempered at 550°C. The presence of hydrogen enhanced stress relaxation, but the effect was also less in the specimen tempered at 650°C. The enhancement by hydrogen is in accord with HELP, but the susceptibility to microstructures is a subject for further studies with respect to microscopic processes of dislocation movement in which hydrogen is involved.

Amorphisation associated with crack growth

The experimental results presented above strongly support a new model of the mechanism of hydrogen related failure that posits that hydrogen enhances the formation of vacancies on straining, thereby reducing ductile crack growth resistance. However, the information has mostly been obtained by means of TDA, and a direct verification is requisite. An expected consequence of a high density of vacancies amounting to $10^{-4}-10^{-5}$ in atomic ratio is either microvoid formation or amorphisation due to lattice instability.[63] Accordingly, deformation microstructures associated with crack propagation in a hydrogen charged ferritic steel have been examined by means of transmission electron microscopy using specimens prepared by the focused ion beam method.[64] As shown in Fig. 21,[64] in the area below the fracture surface, the dislocation density was high, resulting in the formation of cell structures. However, a decrease in the dislocation density and fragmentation of the matrix were observed to take place, leading to the evolution of an amorphous phase in a layer less than 1 μm in thickness adjacent to the surface. Similar structural alterations were also observed eventually within the matrix and in the front of a small crack formed on the side surface of the specimen near the fracture surface, as shown in Fig. 22.[64] The location of the halo rings in Fig. 21*b* suggests that the atomic configuration in the amorphous phase is associated with some lattice expansion. The formation of a high density of vacancies with the aid of hydrogen is likely the cause of amorphisation due to lattice instability and reduced crack growth resistance.

Recently, accelerated fatigue failure in the presence of hydrogen and, conversely, enhanced susceptibility to delayed fracture by fatigue have been demonstrated in high strength steels, together with the formation of vacancies during the fatigue process.[65,66] Strain induced formation of vacancies might play a more significant role in various types of fracture than so far considered.

Conclusions

Recent studies have revealed that plastic straining substantially increases the absorption capacity of weakly trapped hydrogen, the trapping sites of which being ascribed mostly

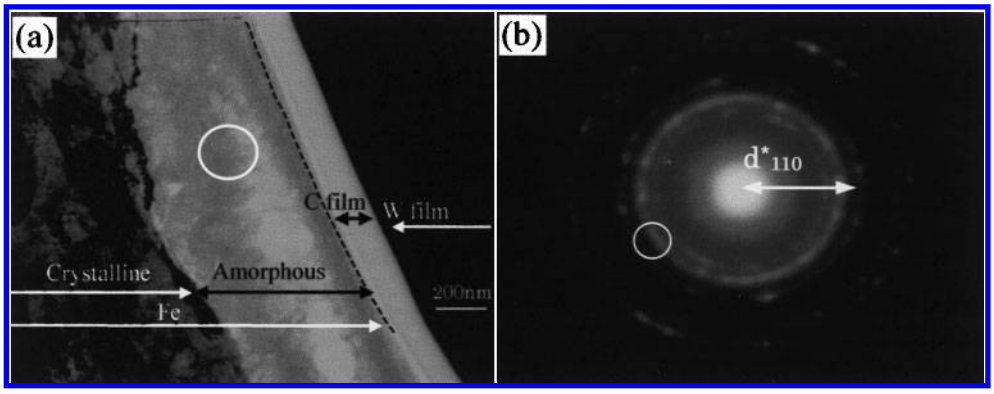

21 *a* amorphous zone developed beneath tensile fracture surface of hydrogen charged ferritic steel; *b* electron diffraction pattern from encircled area in *a*

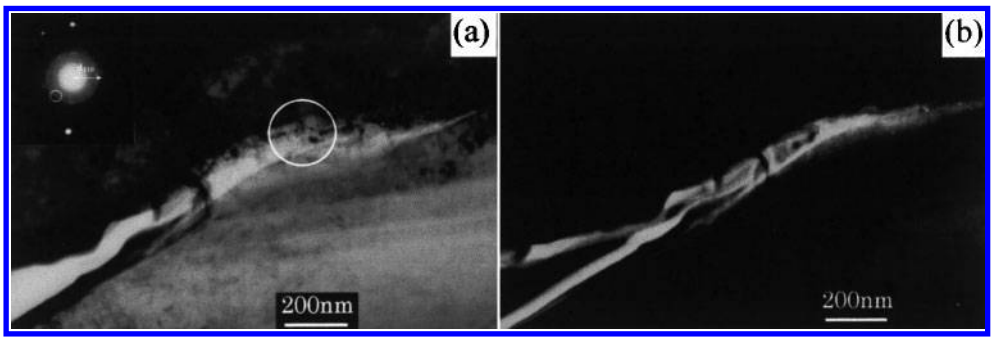

22 *a* grey area developed at front of small side crack; *b* dark field image of same area as *a* from part indicated in diffraction pattern

to vacancies. A correlation between the amount of the increased hydrogen absorption capacity and ductile crack growth resistance was also found. The presence of hydrogen enhanced the increase in strain induced trapping sites and reduced ductile crack growth resistance. The strain induced increase in the hydrogen absorption capacity was correlated with the susceptibility to hydrogen related failure in steels with different microstructures. From these findings, a mechanism of hydrogen related failure has been proposed in which enhanced creation of vacancies and their agglomeration leads to a decrease in ductile crack growth resistance. The new model proposed here was supported by a finding of amorphisation associated with ductile crack growth.

The model shifts the viewpoint concerning the primary factor for degradation from hydrogen itself to vacancies, the formation of which hydrogen enhances. While the observed hydrogen content is very small, the density of vacancies, stabilised by hydrogen, is substantial enough to cause degradation of mechanical properties. Unique fractographic features likely originate in strain concentrated sites such as dislocation cell walls where the formation of vacancies is activated by interactions between dislocations. Nucleation of a high density of voids enhances the localisation of voids at the crack tip, thus leading to shear instability associated with crack advance. The effect of microstructures on susceptibility to hydrogen related failure has been ascribed to the tendency toward vacancy formation on straining, for which the stability of dislocation configurations under stress was suggested as a factor. The accumulation of vacancies might be a cause of the time delay in fracture when hydrogen is involved.

The new concept ranks hydrogen related failure to an extreme case of ductile fracture in which nucleation and linking of cracks is accelerated, but further studies are necessary concerning the effect of vacancy formation on the enhanced mobility of dislocations.

Acknowledgements

The author wishes to express his hearty thanks to Professor H. K. D. H. Bhadeshia of the University of Cambridge for his encouragement to prepare the present article.

References

1. A. S. TETELMAN and W. D. ROBERTSON: *Acta Metall.*, 1963, **11**, 415–426.
2. M. IINO: in 'Hydrogen degradation of ferrous alloys', (ed. R. A. Oriani *et al.*), 737–762; 1985, Park Ridge, NJ, Noyes.
3. J. P. HIRTH: *Metall. Trans. A*, 1980, **11A**, 861–890.
4. S. P. LYNCH: *Acta Metall.*, 1986, **36**, 2639–2661.
5. N. R. MOODY and S. L. ROBINSON: *Res. Mech.*, 1990, **30**, 143–206.
6. H. K. BIRMBAUM: in 'Hydrogen effects on materials behavior', (ed. N. R. Moody and A. W. Thompson), 639–658; 1990, Warrendale PA, TMS.
7. I. M. BERNSTEIN and G. M. PRESOUYRE: in 'Hydrogen degradation of ferrous alloys', (ed. R. A. Oriani *et al.*), 641–658; 1985, Park Ridge N J, Noyes.
8. 'Advances in delayed fracture solution', 1997, Tokyo, Iron and Steel Institute of Japan (in Japanese).
9. 'Functions of hydrogen in environmental degradation of materials 1 – Project Report under the Special Coordination Fund for Promoting Science and Technologies', 2001, The Ministry of Education, Culture, Science, Sports and Technology of Japan (CD–ROM in Japanese).
10. P. KEDZIERZAWSKI: in 'Hydrogen degradation of ferrous alloys', (ed. R. A. Oriani *et al.*), 271–288; 1985, Park Ridge N, Noyes.
11. R. GIBARA and A. J. KUMNICK: in 'Hydrogen embrittlement and stress corrosion cracking', (ed. R. Gibara and R. F. Hehemann), 61–77; 1984, Metals Park, OH, ASM.
12. K. YAMAKAWA, T. TSURUTA and S. YOSHISAWA: *Boshoku-Gijutsu*, 1981, **30**, 501–507.
13. J. P. LAURENT, G. LAPASSET, M. AUCOUTURIER and P. LACOMBE: *Int. J. Appl. Rad. Isot.*, 1973, **24**, 213–230.
14. T. ASAOKA, G. LAPASSET, M. AUCOUTURIER and P. LACOMBE: *Corrosion*, 1978, **34**, 39–47.
15. I. TAGUCHI: *Suppl. Trans. Jpn. Inst. Metals*, 1980, **21**, 225–228.
16. M. AOKI, H. SAITOH, M. MORI, Y. ISHIDA and M. NAGUMO: *J. Jpn. Inst. Met.*, 1994, **10**, 1141–1148.
17. J. OVEJERO-GARCIA: *J. Mater. Sci.*, 1985, **80**, 2623–2629.
18. S. KURAMOTO, K. ICHITANI, A. NAGAO and M. KANNO: *Tétsu-to-Hagané*, 2000, **86**, 17–23.
19. K. ICHITANI, M. KANNO and S. KURAMOTO: *ISIJ Int.*, 2003, **43**, 496–504.
20. W. Y. CHOO and J. Y. LEE: *Metall. Trans. A*, 1982, **13A**, 135–140.
21. K. ONO and M. MESHII: *Acta Metall. Mater.*, 1992, **40**, 1357–1364.
22. M. NAGUMO, K. TAKAI and N. OKUDA: *J. Alloys Compd.*, 1999, **293–295**, 310–316.
23. R. A. ORIANI: *Acta Metall.*, 1970, **18**, 147–157.
24. T. YAMAGUCHI and M. NAGUMO: *ISIJ. Int.*, 2003, **43**, 514–519.
25. M. NAGUMO, K. OHTA and H. SAITOH: *Scr. Mater.*, 1999, **40**, 313–319.
26. N. SUZUKI, N. ISHII and Y. TSUCHIDA: *Tétsu-to-Hagané*, 1994, **80**, 855–859.
27. M. NAGUMO, M. NAKAMURA and K. TAKAI: *Metall. Mater. Trans. A*, 2001, **32A**, 339–347.
28. K. SAKAKI, M. MIZUNO, H. ARAKI, M. HIRATO, M. NAGUMO and Y. SHIRAI: Fall Meeting of Phys. Soc. Japan, Oct. 2003. Details are to be published.
29. M. NAGUMO and K. MIYAMOTO: *J. Jpn. Inst. Met.*, 1981, **45**, 1309–1317.
30. F. TERASAKI, T. KAWAKAMI, A. YOSHIKAWA and N. TAKANO: *Rev. Métall.–CIT/Sci. Génie Matér.*, 1998, 1519–1529.
31. T. J. MARROW, M. AINDOW, P. PRANGNELL, M. STRANGWOOD and J. F. KNOTT: *Acta Mater.*, 1996, **44**, 3125–3140.
32. R. H. VAN STONE, T. B. COX, J. R. LOW JR. and J. A. PSIODA: *Int. Met. Rev.*, 1985, **30**, 157–179.
33. H. G. WILSDORF: *Acta Metall.*, 1982, **30**, 1247–1257.
34. Q.-Z CHEN, W.-Y. CHU, Y.-B. WANG and C.-M. HSIAO: *Acta Metall. Mater.*, 1995, **43**, 4371–4376.
35. A. M. CUTTIÑO and M. ORTIZ: *Acta Mater.*, 1996, **44**, 427–436.
36. M. NAGUMO, T. YAGI and H. SAITOH: *Acta Mater.*, 2000, **48**, 943–951.

37. T. YAGI, A. ITOH and M. NAGUMO: *Tétsu-to-Hagané*, 1995, **81**, 225–230.
38. M. NAGUMO, H. YOSHIDA, Y. SHIMOMURA and T. KADOKURA: *Mater. Trans.*, 2001, **42**, 132–137.
39. A. L. GURSON: *Trans. ASME, J. Eng. Mater. Technol.*, 1977, **99**, 2–15.
40. T. OHMISAWA, S. UCHIYAMA and M. NAGUMO: *J. Alloys Compd.*, 2003, **356–357**, 290–294.
41. Y. FUKAI and N. OKUMA: *Phys. Rev. Lett.*, 1994, **73**, 1640–1647.
42. V. G. GAVRILJUK, V. N. BUGAEV, YU. N. PETROV, A. V. TARASENKO and B. Z. YANCHITSKI: *Scr. Mater.*, 1996, **54**, 903–907.
43. R. B. MCLELLAN and Z. R. XU: *Scr. Mater.*, 1997, **36**, 1201–1205.
44. H. K. BIRNBAUM, C. BUCKLEY, F. ZEIDES, E. SIROIS, P. ROZENAK, S. SPOONER and J. S. LIN: *J. Alloys Compd.*, 1997, **253–254**, 260–264.
45. J. P. HIRTH: in 'Hydrogen effects on materials', (ed. A. W. Thompson and N. R. Moody), 507–522; 1996, Warrendale PA, TMS.
46. K. TAKAI and R. WATANABE: *ISIJ Int.*, 2003, **43**, 520–526.
47. N. SUZUKI, N. ISHII and T. MIYAGAWA: *Tétsu-to-Hagané*, 1996, **82**, 170–175.
48. T. KUSHIDA, N. MATSUMOTO, N. KURATOMI, T. TSUMURA, F. NAKASATO and T. KUDO: *Tétsu-to-Hagané*, 1996, **82**, 297–302.
49. A. R. TROIANO: *Trans. ASM*, 1960, **52**, 54–80.
50. R. A. ORIANI and P. H. JOSEPHIC: *Acta Metall.*, 1974, **22**, 1065–1074.
51. W. W. GERBERICH, R. A. ORIANI, M.-J. LI, X. CHEN and T. FOECKE: *Philos. Mag.*, 1991, **63**, 363–376.
52. M. I. BASKES, C. F. MELIUS and W. D. WILSON: in 'Hydrogen effects in metals', (ed. I. M. Bernstein and A. W. Thompson), 67–74; 1981, Warrendale, PA, AIME.
53. H. K. BIRNBAUM and P. SOFRONIS: *Mater. Sci. Eng. A*, 1994, **A176**, 191–202.
54. P. SOFRONIS and I. M. ROBERTON: *Philos. Mag. A*, 2002, **82**, 3405–3413.
55. P. J. FERREIRA, I. M. ROBERTSON and H. K. BIRNBAUM: *Acta Mater.*, 1999, **47**, 2991–2998.
56. H. A. WRIEDT and R. A. ORIANI: *Acta Metall.*, 1970, **18**, 753–750.
57. P. SOFRONIS and R. M. MCMEEKING: *J. Mech. Phys. Solids*, 1989, **37**, 317–350.
58. J. LUFRANO and P. SOFRONIS: *Acta Mater.*, 1998, **46**, 1519–1526.
59. H. MINAMI, H. FUCHIGAMI and M. NAGUMO: *Curr. Adv. Mater. Process.*, 2001, **14**, 1311.
60. M. NAGUMO and H. MATSUDA: *Philos. Mag. A*, 2002, **82**, 3415–3425.
61. M. NAGUMO, H. UYAMA and M. YOSHISAWA: *Scr. Mater.*, 2001, **44**, 947–952.
62. M. NAGUMO, T. TAMAOKI and T. SUGAWARA: in 'Hydrogen effects on materials behavior and corrosion deformation interactions', (ed. N. R Moody *et al.*); 999–1008, 2003, Warrendale, PA, TMS.
63. R. W. CAHN: *Nature*, 1978, **273**, 491–492.
64. M. NAGUMO, T. ISHIKAWA, T. ENDOH and Y. INOUE: *Scr. Mater.*, 2003, **49**, 837–842.
65. M. NAGUMO, S. SEKIGUCHI, H. HAYASHI and K. TAKAI: *Mater. Sci. Eng. A*, 2003, **A344**, 86–91.
66. M. NAGUMO, H. SHIMURA, T. CHAYA, H. HAYASHI and I. OCHIAI: *Mater. Sci. Eng. A*, 2003, **A348**, 192–200.